

UC Irvine

UC Irvine Previously Published Works

Title

Interactions between polybrominated diphenyl ethers (PBDEs) and TiO₂ nanoparticle in artificial and natural waters.

Permalink

<https://escholarship.org/uc/item/02x3j8dk>

Authors

Wang, Xinzhe
Adeleye, Adeyemi S
Wang, Huihui
et al.

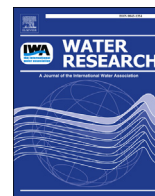
Publication Date

2018-12-01

DOI

10.1016/j.watres.2018.09.019

Peer reviewed



Interactions between polybrominated diphenyl ethers (PBDEs) and TiO₂ nanoparticle in artificial and natural waters

Xinzhe Wang^a, Adeyemi S. Adeleye^{b,1}, Huihui Wang^a, Min Zhang^a, Mengmeng Liu^a, Yingying Wang^a, Yao Li^{a,*}, Arturo A. Keller^{b,**}

^a College of Environmental Science and Engineering/Ministry of Education Key Laboratory of Pollution Processes and Environmental Criteria/Tianjin Key Laboratory of Environmental Remediation and Pollution Control, Nankai University, Tong Yan Road 38, Tianjin 300350, China

^b Bren School of Environmental Science and Management, University of California Santa Barbara, Santa Barbara, CA 93106, United States

ARTICLE INFO

Article history:

Received 11 June 2018

Received in revised form

2 September 2018

Accepted 5 September 2018

Available online 8 September 2018

Keywords:

PBDEs

TiO₂ nanoparticle

Agglomeration

Aqueous media

ABSTRACT

Polybrominated diphenyl ethers (PBDEs) are widely used as flame retardants in a variety of products, including textiles. PBDEs are thus exposed to the natural environment, including wastewater, water-bodies and sediments (at different phases of products' lifecycles), where they will interact with other pollutants. Studies on the interactions between organic pollutants and engineered nanoparticles (NPs) in natural waters are rare. In this study, we investigated the effects of two common PBDEs—BDE 47 and BDE 209—on the physicochemical properties and colloidal stability of TiO₂ NP in simple aqueous media and two natural waters (river water and wastewater). Upon the addition of BDE 47 and BDE 209, the zeta (ζ) potential of TiO₂ NP increased in magnitude in artificial waters and in natural waters (river water and wastewater), but the magnitude of influence on the NP's surface charge was specific to each natural water considered. Despite the presence of high content of natural organic matter in river water (DOC = 15.8 mg/L) and wastewater (DOC = 26.1 mg/L), low levels of the PBDEs (e.g. 0.5 mg/L) strongly impacted the surface charge and hydrodynamic diameter of TiO₂ NP. Both PBDE congeners suppressed the agglomeration of TiO₂ NP in the presence of monovalent and divalent cations, and in both natural waters. BDE 47 exhibited a stronger influence than BDE 209 on the surface charge, hydrodynamic diameter, and agglomeration of TiO₂ NP in both artificial and natural waters. As such, the interactions between TiO₂ NP and the PBDEs can increase the exposure of aquatic organisms to both pollutants. Infrared spectroscopy showed the importance of the aromatic ether groups in the adsorption of PBDEs to TiO₂ NP.

© 2018 Elsevier Ltd. All rights reserved.

1. Introduction

Nanoscale titanium dioxide (TiO₂) is one of the most heavily produced and used engineered nanoparticles (NPs) (Keller et al., 2013). It is often included as a pigment or as the active ingredient in consumer products such as foods and snacks, personal care products, pharmaceuticals, paints, and coatings; and has industrial applications as a catalyst, among others (Chen et al., 2015; Gondikas et al., 2014; Hoffmann et al., 1995). More than 80,000 tons of TiO₂

* Corresponding author.

** Corresponding author.

E-mail addresses: hkliyao@nankai.edu.cn (Y. Li), keller@bren.ucsb.edu (A.A. Keller).

¹ Current address: Department of Civil and Environmental Engineering, University of California Irvine, Irvine, CA 92697, United States.

NP was produced globally in 2010, and a considerable fraction of the TiO₂ NP produced annually ends up in natural aquatic systems (Kaegi et al., 2008; Keller and Lazareva, 2014). Keller and Lazareva (2014) estimated that the concentration of TiO₂ NP in wastewater treatment plants is 5–20 µg/L; and is expected to increase over time with continued increase in the use of the NP (Song et al., 2017). Negative impacts of TiO₂ NP to micro- and macro-organisms and their biochemical processes have been demonstrated over the years (e.g. Bettini et al., 2017; Priester et al., 2014), which underlines the need to thoroughly assess the risk of this widely used NP. Understanding of the fate of TiO₂ NP in aquatic systems is necessary for a reliable environmental risk assessment of the particles in natural waters.

Several studies have investigated the behavior of pristine TiO₂ NP in aqueous systems and the geochemical factors controlling its behavior, such as electrolyte concentration and valence (Adeleye

and Keller, 2016; Domingos et al., 2009; Lin et al., 2017; French et al., 2009; Guzman et al., 2006), media pH (Adeleye and Keller, 2016; Domingos et al., 2009), and natural organic macromolecules (such as fluvic acid and humic acid (Domingos et al., 2009), and extracellular polymeric substances (EPS) (Adeleye and Keller, 2016; Lin et al., 2016, 2017)). Keller and coworkers showed that TiO₂ NP will be completely unstable in natural waters with high ionic strength (e.g. seawater) but may be stable in waters with low salt content and high amount of natural organic matter (NOM) (Keller et al., 2010). In natural waters, the surface of TiO₂ NP will be coated by NOM, including EPS, which can improve the colloidal stability of the NP (Adeleye and Keller, 2016; Domingos et al., 2009; Lin et al., 2016).

Aside from naturally occurring organic compounds (such as NOM), natural waters also contain synthetic organic compounds resulting from direct or indirect anthropogenic pollution. Several studies have shown that NPs can adsorb organic pollutants from water (Vittadini et al., 2000). However, to date few studies have addressed the implications of interactions between organic pollutants and NPs on the environmental fate of NPs. In this study, we chose polybrominated diphenyl ethers (PBDEs) as representative organic pollutants and investigated their influence on the fate of a commercially-sourced TiO₂ NP.

PBDEs have been widely used as flame retardants in paints, plastics, textiles, electronic appliances, and other consumer products (Zhu and Hites, 2004). PBDEs are thus released to the natural environment at different phases of the lifecycle of these products (Branchi et al., 2003; Hale et al., 2003). Although the use of PBDEs has been restricted in several developed countries, these persistent pollutants are still found in products manufactured before the phase-out completion in these countries, and in products made in other parts of the world where the use of PBDEs is unrestricted. PBDEs have been detected in surface waters (including wastewaters, which may have concentrations up to 1000 ng/L) (Peng et al., 2009; U. S. EPA, 2010; Zhang et al., 2009), the atmosphere (Moon et al., 2007), sediments (U. S. EPA, 2010), and humans (Covaci et al., 2008).

We hypothesized that PBDEs will adsorb and concentrate onto the surface of TiO₂ NP in surface waters due to the hydrophobicity of PBDEs and the high surface area of the NP. The objective of this study was to investigate the effect of PBDEs on the physicochemical properties and colloidal stability of TiO₂ NP in both artificial and natural waters. Two widely used congeners of PBDEs, BDE 47 and BDE 209, were selected for this study.

2. Material and methods

2.1. Materials

The TiO₂ NP used in this study has a particle size of 20–50 nm (Fig. 1a), and was purchased from Shanghai Macklin Biochemical Co. (Shanghai, China). The NP is a mixture of anatase (64.2%) and rutile (35.8%), as confirmed via X-ray diffraction analysis (Fig. 1b). Fourier transform infrared (FTIR) spectroscopy (Bruker TENSOR 27, Bruker Optics Inc., Germany) showed a broad intense absorption band in the range of 400–900 cm⁻¹, which is associated with the vibrations of the Ti-O and Ti-O-Ti bonds (Fig. 1c). The band at 1383 cm⁻¹ was attributed to hydroxyl groups while the bands at 1634 and 3402 cm⁻¹ were both attributed to the displacement of weakly adsorbed water molecules. X-ray photoelectron spectroscopy (ESCALAB 250Xi, Thermo Fisher Scientific, Waltham, USA) showed peaks for Ti, O, and C (likely adventitious carbon). The binding energies of Ti 2p, O 1s, and C 1s were 456.0, 531.8 and 285.0 eV, respectively (Fig. 1d). The Brunauer–Emmett–Teller (BET) surface area of the TiO₂ NP, determined using a Micromeritics

ASAP 2010 System, was 64.6 m²/g (Fig. S1).

Two PBDEs, 2,2',4,4'-tetrabromodiphenyl ether (BDE 47) and 2,2',3,3',4,4',5,5',6,6'-decabromodiphenyl ether (BDE 209), were purchased from J & K Scientific Ltd. (Beijing, China), and used for this study. The main physicochemical properties of the PBDEs are shown in Table 1. Stock solutions (500 mg/L) of BDE 47 and BDE 209 were prepared in methanol and tetrahydrofuran (THF), respectively, by mixing with a magnetic stir bar for 2 h. In order to minimize the effects of the solvents, the ratio of solvent: water was kept lower than 1:20 when TiO₂-PBDEs suspensions were prepared for the experiments. More so, preliminary studies showed no significant effects of the solvents on the agglomeration of TiO₂ NP (Fig. S2).

2.2. Preparation of TiO₂ NP suspension

TiO₂ NP stock suspension was prepared via bath sonication. To prepare the stock, 10 mg of pristine TiO₂ NP powder was added to 100 mL deionized (DI) water. The mixture was ultrasonicated in a water bath (Sonics & Material, USA) at 100 W for 120 min. Afterward, the suspension was filtered through a 0.45 μm membrane filter (ANPEL, Shanghai, China) and kept in the dark at room temperature. The TiO₂ NP suspension obtained after filtration had an average hydrodynamic diameter (*D_h*) of 190 nm and a zeta (ζ) potential of -13.3 mV. Both *D_h* and ζ potential were determined using a ZetaSizer Nano ZS90 (Malvern Instruments, Worcestershire, U.K.).

2.3. Effect of PBDEs on the size and surface charge of TiO₂ NP

The stability of NPs is primarily controlled by their surface charges (Israelachvili, 2011). In addition, change in the surface charges of NPs can serve as an indicator of surface interactions with other molecules, ions or particles (Adeleye and Keller, 2013; Adeleye et al., 2016; Israelachvili, 2011). To investigate if there are any interactions between TiO₂ NP and the PBDEs used in this study, we determined the ζ potential of the NP in the presence of BDE 47 and BDE 209 (0–5 mg/L) in DI water at pH 7 (achieved by adding negligible amounts of dilute HCl and/or NaOH). These concentrations of PBDE exceed what is typically detected in natural waters but highly hydrophobic organic compounds usually concentrate on the surface of solid particles in water as explained in detail later. Measurements in DI water enabled us to clearly observe trends without the interference of other materials. Additional ζ potential measurements were carried out in two natural waters—river water and wastewater—to determine if similar effects would be observed as in DI water. The river water was collected from South Pai River (Tianjin, China) while the wastewater was a secondary effluent obtained from Tianjin Four East Sewage Treatment Plant, China. Both natural waters were filtered through a 0.45 μm mixed cellulose esters membrane filter (Xingya Company, Shanghai, China). The major properties of the natural waters are shown in Table S1. The ζ potential of TiO₂ NP was measured in triplicates for each concentration of PBDE. In addition, the size of TiO₂ NP was determined in the presence of BDE 47 and BDE 209 both in DI and the two natural waters, to see the effect of the PBDEs on the *D_h* of TiO₂ NP.

2.4. Agglomeration kinetics experiments

2.4.1. Simple salt solutions

TiO₂ NP agglomeration was studied at 20 °C via time-resolved dynamic light scattering (TR-DLS) using the Zetasizer (Li et al., 2016; Qi et al., 2016). For this analysis, the TiO₂ NP stock suspension was sonicated for 30 min after which a pre-determined amount of the stock was then pipetted into a glass vial containing

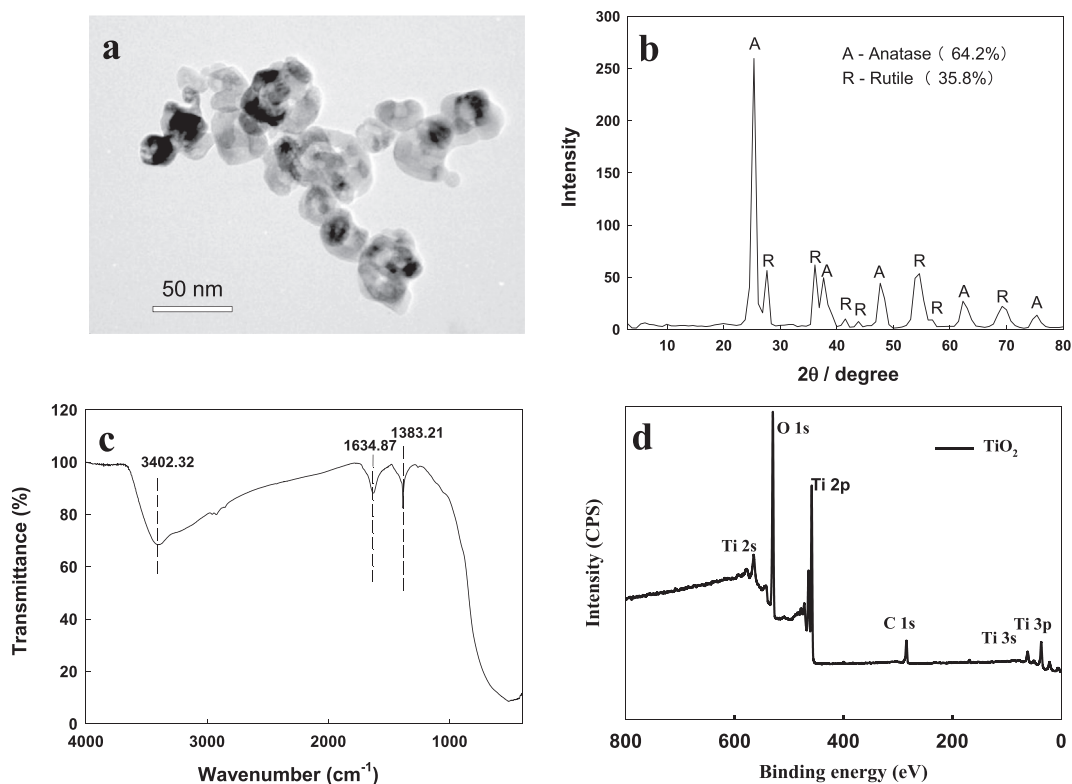
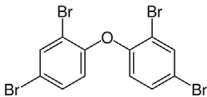
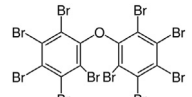


Fig. 1. Characterization of the TiO₂ nanoparticles used in this study. (a) TEM micrograph, (b) XRD spectrum, (c) FTIR spectrum, (d) XPS survey spectrum of TiO₂ nanoparticles.

Table 1
Important physicochemical properties of the PBDEs used in this study.

Property	BDE 47	BDE 209
Solubility (μg/L)	1–15	20–30
Log K _{ow}	6.77–6.81	6.27–9.97
Molecular weight (g/mol)	485.8	959.2
Molecular structure		

Sources: EPA 2010 (Hua et al., 2003; Tittlemier et al., 2002; U. S. EPA, 2010)

a known volume of either DI water or an electrolyte stock solution (NaCl, KCl, CaCl₂ or MgCl₂). The pH of the respective suspensions obtained was thereafter adjusted with 0.1 mM NaOH or HCl. The vial was capped and immediately vortexed for 5 s to mix. After mixing, 1 mL of the suspension was pipetted into a polystyrene cuvette, which was then placed in the Zetasizer sample chamber for analysis. For studies investigating the influence of PBDEs on the agglomeration kinetics of TiO₂ NP, known amounts of BDE 47 or BDE 209 stock solutions were pipetted into the glass vial before the addition of TiO₂ NP. TR-DLS data were collected in triplicates at 15 s intervals for 40 min. Final TiO₂ NP concentration was 10 mg/L to obtain sufficient signal for TR-DLS analysis.

2.4.2. Theory and data analysis

The initial agglomeration period was defined as the time from when the TR-DLS experiment was initiated (t_0) to the time when the measured hydrodynamic diameter (D_h) value reached about 1.3 times the initial D_h . The initial agglomeration rate constant of TiO₂ NP (k_a) is proportional to the initial rate of increase in D_h with time (t), and the inverse of TiO₂ NP concentration (N_0) (Adeleye and

Keller, 2013; Adeleye et al., 2014; Chen and Elimelech, 2006):

$$k_a \propto \frac{1}{N_0} \left(\frac{dD_h(t)}{dt} \right)_{t \rightarrow 0} \quad (1)$$

The particle attachment efficiency, α , (or inverse stability ratio, $1/W$) was used to quantify TiO₂ NP agglomeration kinetics in simple media, and was calculated by normalizing the initial agglomeration rate constant (k_a) with the agglomeration rate constant measured under diffusion limited (fast) conditions:

$$\alpha = \frac{1}{W} = \frac{k_a}{k_{a,fast}} = \frac{\frac{1}{N_0} \left(\frac{dD_h(t)}{dt} \right)_{t \rightarrow 0}}{\frac{1}{(N_0)_{fast}} \left(\frac{dD_h(t)}{dt} \right)_{t \rightarrow 0, fast}} \quad (2)$$

where the subscript “fast” represents favorable solution conditions, where fast, diffusion-limited agglomeration takes place (Chen and Elimelech, 2006).

Critical coagulation concentration (CCC) of NaCl for GO NP was determined from the intersection of extrapolated lines through the diffusion- and reaction-limited regimes (Bouchard et al., 2009; Chowdhury et al., 2013). The CCC, which represents the minimum amount of an electrolyte needed to completely destabilize a NP in aqueous media, provides a useful metric of colloidal stability for NPs and hence can be used in the prediction of the fate and transport of NPs in natural waters (Adeleye and Keller, 2013, 2016; Zhou et al., 2013).

2.4.3. Natural waters

Agglomeration kinetics of TiO₂ NP was also investigated in river water and wastewater to relate well-controlled simple solution chemistries to more complex, environmentally-relevant conditions. The initial agglomeration rate constant of TiO₂ NP (k_a) in river

water and wastewater was determined via TR-DLS technique as described earlier (Eq. (1)). Final TiO_2 NP concentration was 10 mg/L to obtain sufficient signal for TR-DLS analysis, and the concentrations of PBDEs were varied between 0 and 10 mg/L.

2.5. Spectroscopic investigation of PBDE- TiO_2 NP interactions

FTIR spectroscopy was used to probe interactions between the PBDEs and TiO_2 NP using the 110 Bruker TENSOR 27 in transmission mode. TiO_2 NP and the PBDEs were analyzed separately, and after mixing them together in suspension. To prepare samples for analysis, the suspensions of TiO_2 NP and PBDEs were freeze dried. Interferograms were obtained by collecting 100 scans at a resolution of 4 cm^{-1} . In addition to FTIR, XPS analysis was conducted (using the ESCALAB 250Xi) to confirm the presence of different elements and functional groups before and after mixing TiO_2 NP and PBDEs.

3. Results and discussion

3.1. Effects of PBDEs on the surface charge of TiO_2 NP

The ζ potential of TiO_2 (10 mg/L NP dispersion) at pH 7 was -13.3 mV . The isoelectric point of TiO_2 NP that contains anatase and rutile is $\sim\text{pH } 5\text{--}6$ (Jallouli et al., 2014; Zhou et al., 2013), thus, TiO_2 NP are slightly negatively charged at pH 7. Upon the addition of BDE 47 and BDE 209, the ζ potential of TiO_2 NP increased in magnitude (became more negative) as shown in Fig. 2a. More importantly, the ζ potential of TiO_2 NP further increased in magnitude with higher concentrations of the PBDEs. For instance, the ζ potential of TiO_2 NP increased in magnitude from -13.3 mV in DI water to -33.2 mV in the presence of 5 mg/L BDE 47 and to -27.1 mV in the presence of 5 mg/L BDE 209. It is

noteworthy that the ζ potential of 5 mg/L BDE 47 was measured as -53.0 mV while the ζ potential of 5 mg/L BDE 209 was found to be -46.8 mV in DI water (pH 7).

Our result shows the surface charge of TiO_2 NP shifted towards that of the PBDEs upon the addition of increasing amounts of the organic compounds. This suggests that the PBDEs, like several natural organic molecules (Adeleye and Keller, 2016; Domingos et al., 2009; Lin et al., 2016), can interact with the surface of the TiO_2 NP. In addition, the interactions with the PBDEs increased the net surface charge of the TiO_2 NP. Since the colloidal stability of NPs increase with increase in the magnitude of their surface charge, we hypothesized that the colloidal stability of TiO_2 NP will increase in the presence of BDE 47 and BDE 209. In addition, the presence of BDE 47 and BDE 209 may confer steric stability on the TiO_2 NP as well.

Assuming the PBDEs, at 5 mg/L, were completely adsorbed onto the surface of TiO_2 NP, the amount of BDE 47 on the surface of the particles would be $1.59\text{ }\mu\text{mol-PBDE}/\text{m}^2\text{-TiO}_2$ while the amount of BDE 209 on the surface of TiO_2 particles would be $0.81\text{ }\mu\text{mol-PBDE}/\text{m}^2\text{-TiO}_2$. In other words, there was about twice as many molecules of BDE 47 as of BDE 209 on the surface of TiO_2 NP when equal mass concentrations of both PBDEs were added into TiO_2 NP suspensions. We therefore hypothesized that BDE 47 will improve the colloidal stability of TiO_2 NP much better than BDE 209 due to BDE 47's greater electrostatic (Fig. 2a) and steric stabilization (originating from greater NP surface coating).

The presence of electrolytes ($0\text{--}30\text{ mM Na}^+$ and $0\text{--}0.5\text{ mM Ca}^{2+}$) decreased the magnitude of the surface charge of TiO_2 NP with or without BDE 47 and BDE 209, due to the accumulation of the positively charged ions around the electric double layer of the particle, screening the surface charge of the NP (Fig. 2b–c). As an example, the ζ potential of TiO_2 NP with 10 mg/L BDE 47 changed

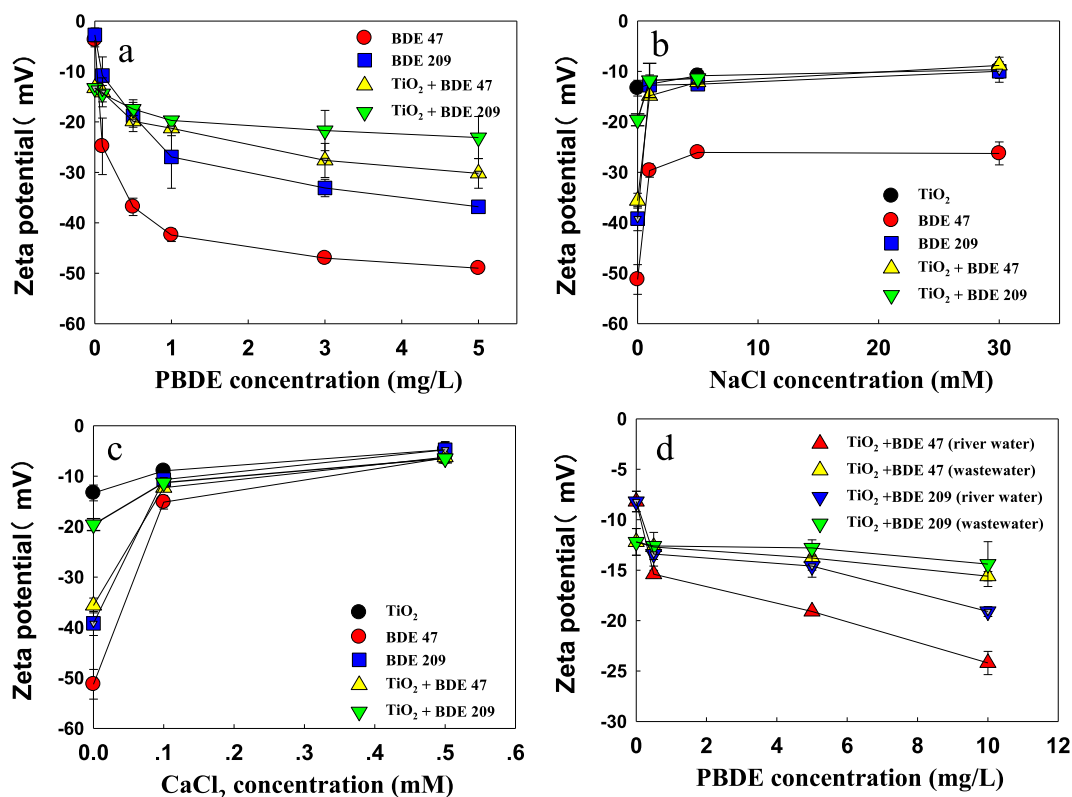


Fig. 2. Zeta potential of (a) TiO_2 nanoparticles with PBDEs (0–5 mg/L) in DI water. Zeta potential of TiO_2 nanoparticles, PBDEs and TiO_2 nanoparticles coated with PBDEs in (b) NaCl and (c) CaCl_2 solutions. The zeta potential of TiO_2 nanoparticles coated with PBDEs in the river water and wastewater is shown in (d).

from -35.6 mV in DI to -14.8 mV in the presence of 1 mM NaCl. The effect of Ca^{2+} on ζ potential was even more pronounced as it only required 0.1 mM CaCl_2 to decrease the magnitude of ζ potential of TiO_2 NP with 10 mg/L BDE 47 to -12.3 mV. This agrees with the Schulze-Hardy rule that higher valence cations have higher charge screening capability. A similar trend was observed when the ζ potential of TiO_2 NP only or the PBDEs by themselves were measured in the presence of the electrolytes (Fig. 2b–c). It is also noteworthy that for Na^+ , the effect on ζ potential of TiO_2 NP was stronger between 0 and 1 mM of the cation than between 1 and 30 mM. Similarly, the strongest effect of Ca^{2+} on ζ potential was observed at 0.1 mM; and further changes in ζ potential when Ca^{2+} was increased by five times was not proportional to the increase in electrolyte concentration.

In the natural waters, the average ζ potential of TiO_2 NP was -8.2 mV in river water and -12.2 mV in wastewater. The charge on the surface of TiO_2 NP in these natural waters was controlled by interactions between the NP and the natural organic materials (which increase the negative charge on the surface of TiO_2 NP (Adeleye and Keller, 2016; Keller et al., 2010)) and ions (with cations screening the electrostatic charge on the surface of TiO_2 NP (Adeleye and Keller, 2016; Keller et al., 2010)). Despite the presence of these existing strong surface interactions, the ζ potential of TiO_2 NP was impacted by BDE 47 and BDE 209 even at PBDE concentrations as low as 0.5 mg/L (Fig. 2d). We observed an increase in the magnitude of the ζ potential of TiO_2 NP upon the addition of BDE 47 and BDE 209 in both river water and wastewater, albeit to different degrees. For instance, the ζ potential of suspension of TiO_2 NP in river water increased in magnitude from -8.2 mV to -15.4 mV upon the addition of 0.5 mg/L BDE 47. Further increase in BDE 47 concentration resulted in further increase in magnitude of the surface charge of the TiO_2 NP. At 10 mg/L PBDE concentrations we observed a ζ potential of -24.2 mV (BDE 47) or -19.1 mV (BDE 209). A similar trend was observed in the presence of the PBDEs when TiO_2 NP suspension was prepared in wastewater. However, the PBDEs had much more impact on the ζ potential of TiO_2 NP in river water than in wastewater. This suggests that PBDEs, even at low concentrations, can influence the surface charge of TiO_2 NP in different waters, but the magnitude of the impact may be differ based on the water chemistry. Changes in the surface charge of TiO_2 NP in natural waters, induced by the PBDEs may influence the interactions of the NP with other materials (geological, biological or chemical) present in water, and impact the fate and transport of the NP.

3.2. Effects of PBDEs on the hydrodynamic size of TiO_2 NP

As mentioned earlier, D_h of the TiO_2 NP in DI water was determined as 190 nm, which is larger than the reported primary particle size (20 – 50 nm). The larger size observed in DI water indicates that the NP existed as agglomerates in water, to reduce the high surface energy inherent to nanosized particles (Adeleye et al., 2014; Keller et al., 2010; Zhou et al., 2013). More so, DLS analysis considers any solvent molecules attached to the surface of the NP within the media. Upon the addition of BDE 47 and BDE 209, the D_h of TiO_2 NP increased (from 190 nm) to 200 nm and 240 nm, respectively (Fig. 3a). The number-based size distribution of TiO_2 NP in DI water (Fig. 3b) shows that most of the particles have a size range of 160 – 220 nm. As shown in Fig. 3c–d, the size distribution of TiO_2 NP upon the addition of BDE 47 (170 – 230 nm) was similar to the size distribution of the NP in DI water. However, the size distribution of the NP shifted slightly to a larger size range (190 – 280 nm) upon the addition of BDE 209.

An increase in D_h /size distribution of NPs in media typically indicates (1) increased particle agglomeration, or (2) particle

coating (Adeleye et al., 2014, 2016). The increase in size and size distribution of TiO_2 NP upon the addition of PBDEs (particularly BDE 209) was due to the coating of the particles by the organic pollutants. Only a slight increase in D_h /size distribution was observed in the presence of BDE 47 due to its small size (molecular weight = 485.5 g/mol) compared to BDE 209, which is almost twice as large (molecular weight = 959.2 g/mol). An increase in the proportion of particles with size range 240 – 250 nm in the presence of BDE 209 (compared to BDE 47 and DI water) may also suggest a lower colloidal stability of TiO_2 NP in the presence of BDE 209 than in DI water and BDE 47. To confirm, agglomeration studies were carried out in the presence of electrolytes, as discussed in the next section.

The D_h of TiO_2 NP increased from 190 nm in DI to 659 nm in the river water, and 769 nm in the wastewater (Fig. 4a). This is mainly due to high salt content of both waters as indicated by their relatively high conductivities (1473 $\mu\text{S}/\text{cm}$ for river water and 4509 $\mu\text{S}/\text{cm}$ for wastewater) compared to DI. As shown in Figs. 4b and S3a, the TiO_2 NP agglomerated to a size range of 400 – 750 nm in river water, and 400 – 950 nm in wastewater (in the absence of the PBDEs). The addition of both BDE 47 and BDE 209 improved the stability of the NP as shown by the decrease in D_h (Fig. 4a) and number-based size distribution (Fig. 4c–d and S3–S5) at all PBDE concentrations tested. For instance, D_h of the TiO_2 NP decreased to 457 nm in river water and 653 nm in wastewater when 0.5 mg/L BDE 47 was present. This observation agrees well with ζ potential measurements, which also showed a clear influence even at low levels of the PBDEs in natural waters despite the presence of relatively high content of NOM (Table S1). In agreement with ζ potential measurements, the decrease in the D_h of TiO_2 NP was more drastic in the presence of (increasing amounts of) BDE 47 than in the presence of (increasing amounts of) BDE 209 (Fig. 4a). The shift in size range of TiO_2 NP to smaller sizes when coated by PBDEs in natural waters can increase the probability of PBDE-coated TiO_2 NP being taken up by organisms. As such, the interactions between TiO_2 NP and the PBDEs can increase the exposure of aquatic organisms to both pollutants.

3.3. Effects of PBDEs on TiO_2 NP agglomeration kinetics

To quantitatively evaluate the stabilizing effects of BDE 47 and BDE 209 on TiO_2 NP in aqueous media, the agglomeration kinetics of TiO_2 NP was studied at 30 mM NaCl in the presence of both PBDEs. The PBDEs were added in increasing amount until the agglomeration of TiO_2 NP was fully suppressed. Although both BDE 47 and BDE 209 stabilized TiO_2 NP in aqueous media, the patterns of stabilization were quite different.

TiO_2 NP was unstable at 30 mM NaCl as shown by an increase in D_h from 250 nm to ~ 600 nm within 30 min (Fig. S6). Upon the addition of 0.1 mg/L BDE 47 the agglomeration of TiO_2 NP was slightly suppressed, with D_h only reaching ~ 500 nm over a period of 30 min. Agglomeration of TiO_2 NP was increasingly suppressed with the addition of increasing amounts of BDE 47, and complete suppression of TiO_2 NP in 30 mM NaCl was observed in the presence of 5 mg/L BDE 47. Conversely, there was either no or minimal suppression of TiO_2 NP agglomeration even up to 5 mg/L BDE 209 at this ionic strength. In fact, agglomeration of TiO_2 NP was slightly suppressed at 0.1 mg/L and 0.5 mg/L BDE 209 above which the agglomeration rate of TiO_2 NP increased again. The D_h of TiO_2 NP exceeded 600 nm after 30 min in the presence of 5 mg/L BDE 209. Surprisingly, at BDE concentrations above 5 mg/L the agglomeration of TiO_2 NP was almost completely suppressed by BDE 209 in 30 mM NaCl and pH 7 (Fig. S7). The requirement of a higher amount of BDE 209 than BDE 47 to suppress the agglomeration of TiO_2 NP at a similar ionic strength confirms that BDE 47 is a better stabilizer of

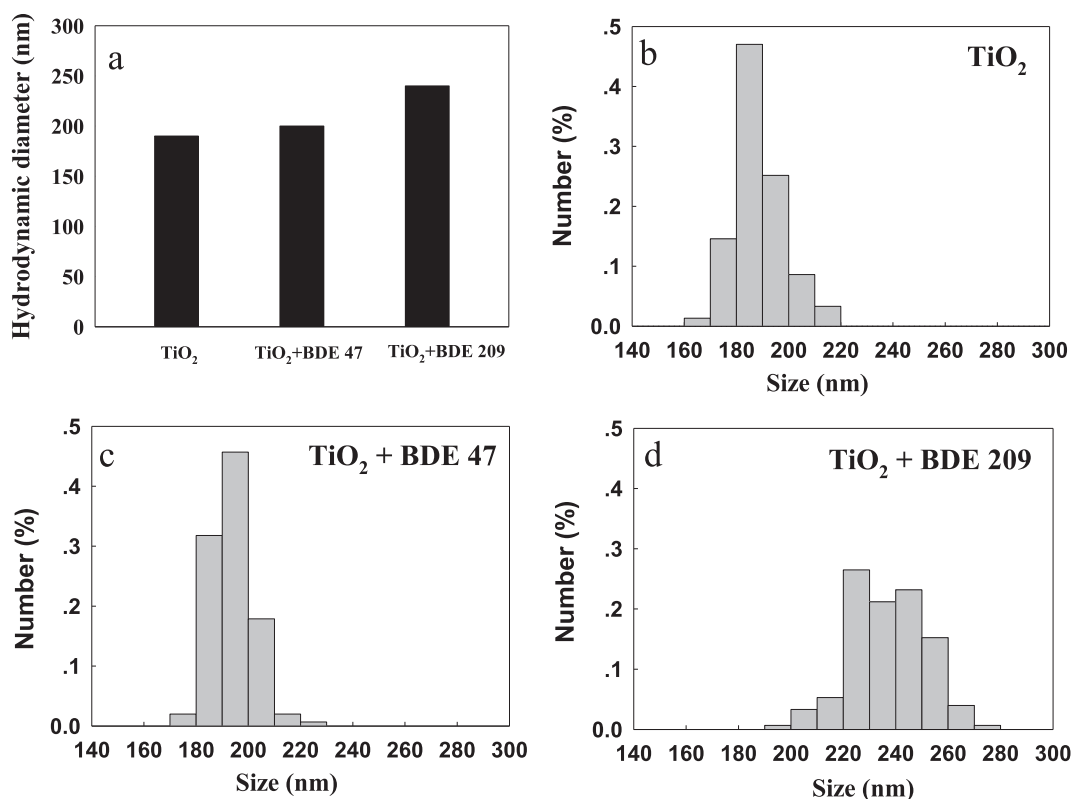


Fig. 3. Size of TiO_2 nanoparticles in simple media. (a) Hydrodynamic diameter (D_h) of TiO_2 nanoparticles with or without PBDEs (3 mg/L) in DI water. Number-based size distribution of (b) TiO_2 nanoparticles suspension in DI water, (c) suspension of TiO_2 nanoparticles with 3 mg/L of BDE 47, and (d) suspension of TiO_2 nanoparticles with 3 mg/L of BDE 209. For all experiments, TiO_2 nanoparticles = 10 mg/L and pH = 7.

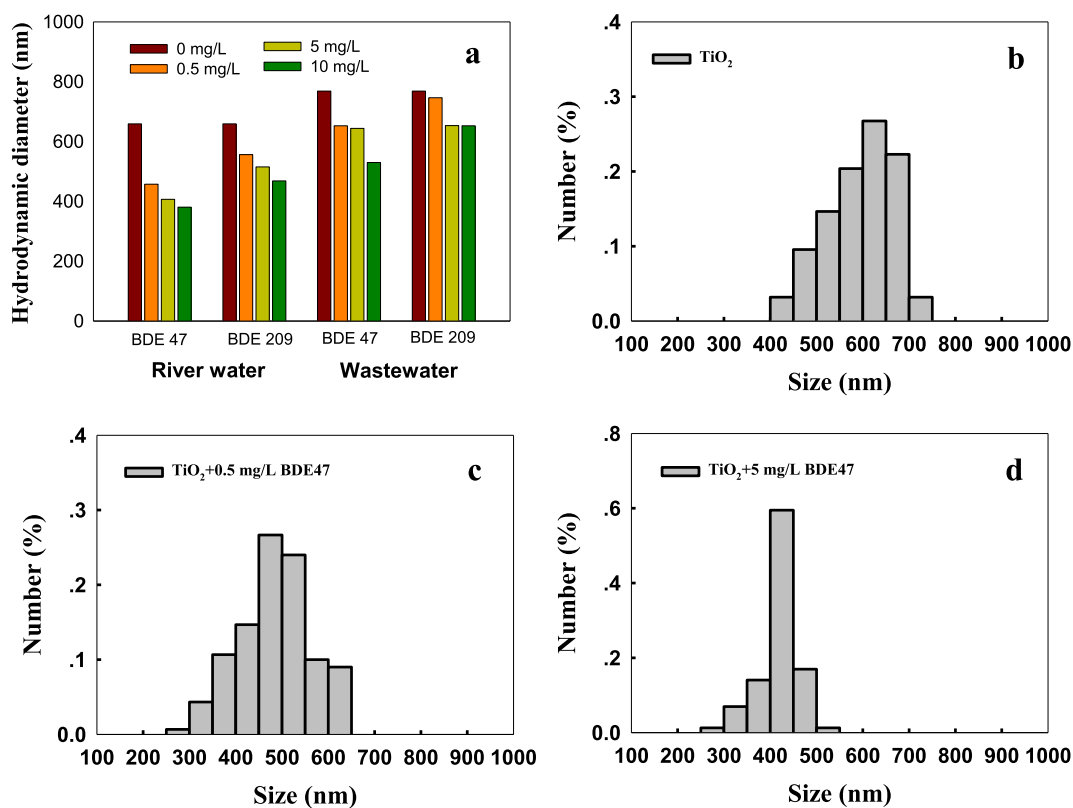


Fig. 4. Size of TiO_2 nanoparticles in natural waters. (a) Hydrodynamic diameter (D_h) of TiO_2 nanoparticles with PBDEs (0, 0.5, 5, 10 mg/L) in river water and wastewater. Number-based size distribution of (b) TiO_2 nanoparticles only (c) TiO_2 nanoparticles with 0.5 mg/L BDE 47 and (d) TiO_2 nanoparticles with 5 mg/L of BDE 47 in river water samples.

TiO₂ NP, especially at low PBDE concentrations. This observation of a better stabilizing potential of BDE 47 agrees with our earlier observation that BDE 47 imparted a higher surface charge and a more effective surface coating of TiO₂ NP than BDE 209.

Initial agglomeration rates (k_a) were determined from the kinetics (TR-DLS) data. The k_a of TiO₂ NP decreased from 9.65 nm/min in the absence of the PBDEs to 0.57 nm/min when the concentration of BDE 47 reached 5 mg/L. As stated earlier, TiO₂ NP was not stable in BDE 209 until the concentration of the organic contaminant exceeded 5 mg/L. Surprisingly, the k_a of TiO₂ NP decreased slightly from 9.65 nm/min in the absence of BDE 209 to 9.4 nm/min and 8.8 nm/min in the presence of 0.1 mg/L BDE 209 and 0.5 mg/L BDE 209, respectively. The adsorption of PBDEs from aqueous phase onto solids may occur via electrostatic attraction and can thus be influenced by pH and ionic strength (Ni et al., 2014). Additionally, cations can compete with PBDEs for adsorption, and competitive binding increases with hydrophobicity. We suspect that 30 mM NaCl affected the effective binding of BDE 209 onto the surface of TiO₂ NP, but the effect was minimal for the smaller and less hydrophobic BDE 47 and at higher concentrations of BDE 209 (>5 mg/L).

The agglomeration kinetics data of TiO₂ NP in the natural waters with and without the PBDEs are presented in Fig. S8. In the natural waters, both BDE 47 and BDE 209 decreased the agglomeration rate of TiO₂ NP as shown by the k_a values presented in Fig. 5a and b. For instance, the k_a of TiO₂ NP decrease from 23.8 nm/min in pristine river water (DOC = 15.8 mg/L) to 10.4 nm/min upon the addition of 0.5 mg/L BDE 47. Further decrease was observed with additional amounts of BDE 47, and k_a decreased to 8.95 nm/min in the presence of 10 mg/L BDE 47. We observed similar trends for BDE 47 in wastewater and BDE 209 in both types of natural waters. It is thus

clear that even in the presence of abundant naturally occurring organic materials, anthropogenic organic pollutants like the PBDEs can strongly influence the environmental fate of TiO₂ NP, even when the pollutants are present at concentrations much lower than naturally occurring organic materials.

PBDE congeners have a very low aqueous solubility (1–30 µg/L) in water, hence, it is unlikely that TiO₂ NP will be released into a water body that contains PBDEs levels that will fully stabilize TiO₂ NP in natural waters. The extremely high hydrophobicity of BDE 47 (log K_{ow} = 6.77–6.81) and BDE 209 (log K_{ow} = 6.27–9.97) will promote their partitioning out of the aqueous phase onto the surface of TiO₂ NP in natural waters—making the NP act as a sorbent (Hua et al., 2003). As such, although the nominal concentration of PBDEs and other organic contaminants in water may be very low, the surface of TiO₂ NP (and possibly other metallic NPs) may be effectively covered by these hydrophobic organic compounds in natural waters, which as shown here can influence the colloidal stability of the NP.

The interactions between TiO₂ NP and PBDEs may occur via electrostatic forces due to their respective surface charges, physical interactions, and perhaps, chemical bonding. Physical interactions such as Van der Waals and hydrophobic interactions, and hydrogen bonding between surface Ti-OH groups (donor) of the NP and ether (-O-) groups in PBDEs (acceptor), or induced dipole may be responsible for interactions between TiO₂ NP and PBDEs (Li et al., 2010; Vargas and Núñez, 2009). FTIR spectra of TiO₂ NP before and after interactions with the PBDEs were collected. As can be seen in Fig. 5c and d, the spectra of TiO₂ NP before and after interactions with BDE 47 and BDE 209 were quite similar. However, a new peak around 1331 cm⁻¹ was observed after TiO₂ NP was mixed with and allowed to interact with either PBDE. The peak around

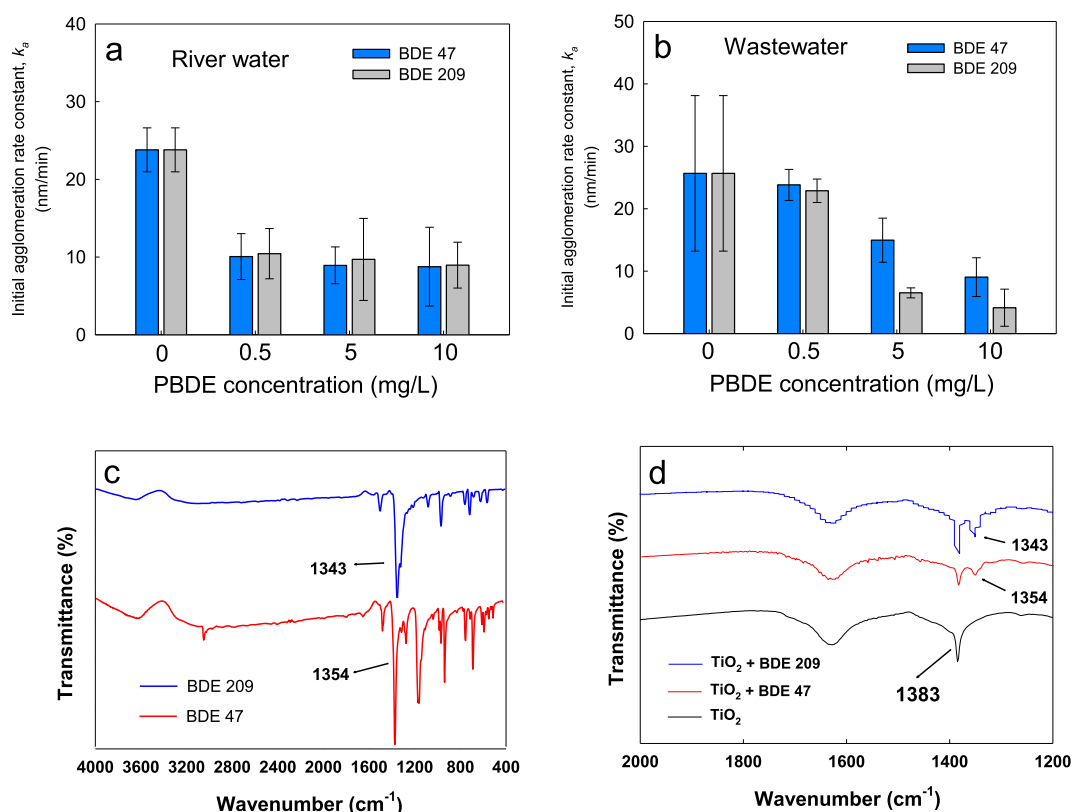


Fig. 5. Initial agglomeration rate constant (k_a) of TiO₂ nanoparticles at different concentrations of PBDE in (a) river water and (b) wastewater. FTIR spectra of (c) BDE 47 and BDE 209, and (d) TiO₂ nanoparticles coated with BDE 47 and BDE 209.

1331 cm^{-1} may be assigned to the aromatic ether ($-\text{O}-$) groups on PBDEs (Lambert et al., 1987; Peng et al., 2013). This peak confirms the adsorption of the PBDEs onto the surface of TiO_2 NP and shows the importance of the aromatic ether bond present in BDE 47 and BDE 209 for the adsorption of the PBDEs to TiO_2 NP. In addition, following particle recovery and drying, XPS analysis showed the presence of Br on the surface of TiO_2 NP after allowing the NP to interact with BDE 47 and BDE 209 in suspension (Fig. 6).

3.4. Effects of PBDEs on TiO_2 colloidal stability

To further characterize the effects of the PBDEs on the stability of TiO_2 NP, the influence of the PBDEs on the CCC of NaCl for TiO_2 NP was determined. At the CCC, and electrolyte concentrations above the CCC, the energy barrier between particles is eliminated, leading to diffusion-controlled agglomeration. We determined the CCC of NaCl for TiO_2 NP with and without the PBDEs in simple media. For comparison, the effects of Suwannee River humic acid (SRHA), a commonly used proxy for natural organic matter, was also determined.

As shown in Fig. S9, distinct diffusion-limited agglomeration and reaction-limited agglomeration regimes were observed with and without the PBDEs. The observed CCC of NaCl for the TiO_2 NP at pH 7 was 1.2 mM. Natural freshwaters typically have ionic strengths of 1–15 mM (Conway et al., 2015), so the bare TiO_2 NP used in this study will likely settle out to the sediment phase if released into a natural water (unless they adsorb organic materials in water). However, the CCC of the TiO_2 NP increased to 8.6 mM NaCl in the presence of 0.5 mg/L BDE 47, and to 4.8 mM NaCl in the presence of 0.5 mg/L BDE 209. This slight increase in CCC implies an

improvement in the stability of the TiO_2 NP in natural freshwaters. Thus, the adsorption of PBDEs on the surface of TiO_2 NP, even at low concentrations can change the fate of TiO_2 NP in freshwaters, making them more likely to be present in the water column than in the sediment zone. SRHA increased the CCC of NaCl for TiO_2 NP by two orders of magnitude, to 101.5 mM NaCl.

Due to the peculiar behavior of BDE 209 (little or no suppression of k_d at 0–5 mg/L, Fig. S6), further experiments were conducted to determine the CCC of NaCl for TiO_2 NP in the presence of BDE 209 above and below 5 mg/L. The CCC increased slightly from 4.8 mM NaCl to 5.4 mM NaCl when the concentration of BDE 209 increased from 0.5 mg/L to 3 mg/L (Fig. S9b). However, the CCC was 78.9 mM NaCl when the concentration of BDE 209 reached 6 mg/L. These findings agree with the k_d data which only showed a remarkable improvement in the stability of TiO_2 NP when the concentration of BDE 209 exceeded 5 mg/L.

According to the Derjaguin-Landau-Verwey-Overbeek (DLVO) theory, increasing ionic strength reduces the electrostatic energy barrier and deepens the secondary minimum well, which promotes agglomeration due to increase in attachment efficiency (Ambrosi et al., 2012). Thus, the behavior of TiO_2 NP in the presence of NaCl followed the DLVO theory. However, while the classical DLVO theory includes electric double layer and van der Waals interactions, it may not accurately capture NP behavior when coated by an organic compound, as the coating may result in steric repulsion forces (Wang et al., 2015). SRHA is a complex heterogeneous macromolecule made up of aliphatic and aromatic hydrocarbons. SRHA has a weight-averaged molecular weight (M_w) of 3400 Da (Her et al., 2002; Wang et al., 2015), thus, much larger than the PBDEs. In addition, unlike the PBDEs, SRHA contains numerous

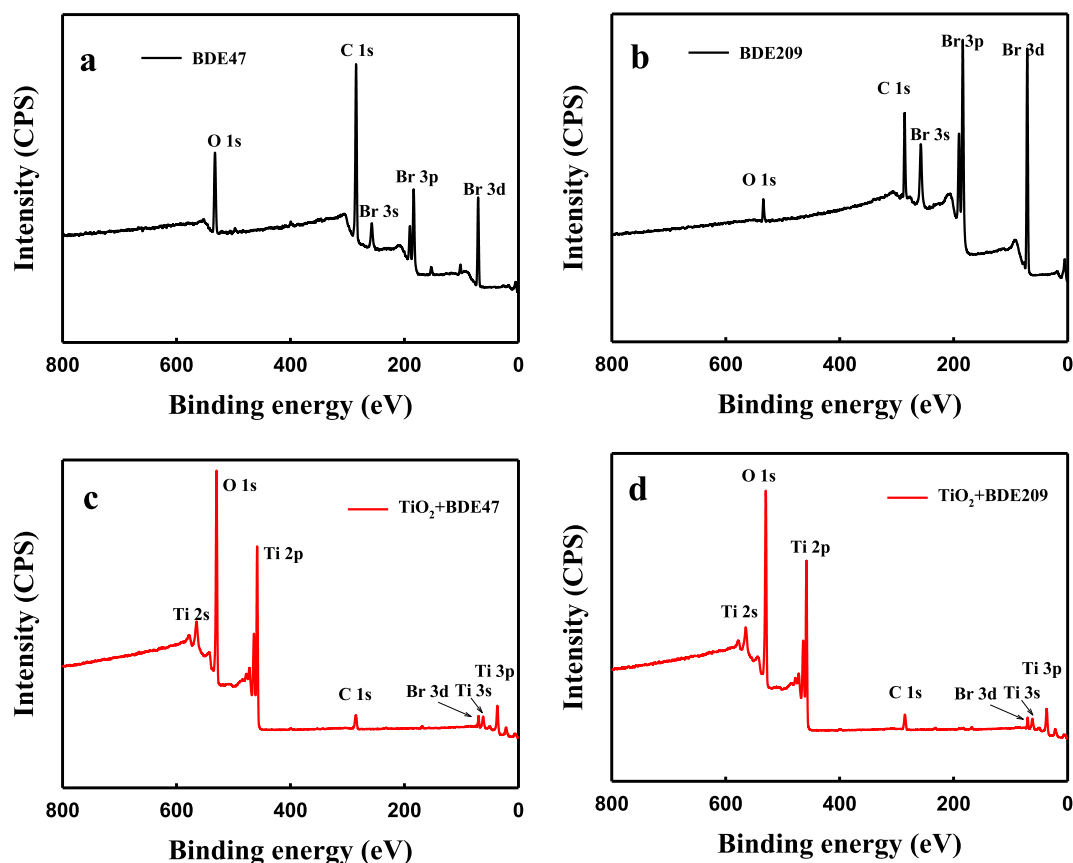


Fig. 6. XPS survey spectra of (a) BDE 47, (b) BDE 209, (c) TiO_2 NPs coated with BDE 47 and (d) TiO_2 NPs coated with BDE 209. The presence of Br in (c) and (d) confirms the adsorption of the PBDEs on TiO_2 nanoparticles.

functional groups including amide, carboxyl, hydroxyl, ketone, etc. (Adeleye et al., 2014; Leenheer and Croué, 2003). SRHA is known to effectively adsorb to TiO_2 NP and stabilize it via electrostatic repulsion and steric hindrance (Adeleye and Keller, 2016; Wang et al., 2016), and as shown here, much more so than PBDEs.

3.5. Effects of cation species on agglomeration kinetics

The effects of BDE 47 and BDE 209 on the agglomeration kinetics of TiO_2 NP in the presence of different cation species were tested using K^+ and Na^+ as monovalent cations, and Ca^{2+} and Mg^{2+} as divalent cations. Divalent cations typically have larger destabilizing effects than monovalent cations on NP suspensions due to the greater charge screening effects of divalent ions than monovalent ions, as described by classical colloidal theory (Ambrosi et al., 2012). This additional study was conducted to see if the interactions among TiO_2 NP, cations of different valences, and PBDEs have any effects on the agglomeration behavior of the NP.

The CCC of TiO_2 NP used in this study is 1.2 mM NaCl (Fig. S9) and as expected, the NP agglomerated rapidly at 1 mM of the monovalent ions (Fig. 7a) due to the proximity of α to unity in these conditions. As expected, the NP was completely unstable at 5 mM NaCl and KCl. The impact of Na^+ and K^+ on the agglomeration of NPs are often similar although some researchers have reported that K^+ resulted in slightly more agglomeration due to its larger size and smaller hydration shell thickness (e.g. Yang et al., 2016). Here, the k_a values of TiO_2 NP were similar in the presence of Na^+ or K^+ at 1 mM (5.9 nm/min and 4.2 nm/min respectively) and 5 mM (10.8 nm/min and 10.9 nm/min respectively).

Ca^{2+} (ionic radius = 0.99 Å) typically destabilizes NPs more than Mg^{2+} (ionic radius = 0.65 Å) because of the larger size, smaller hydration shell thickness and the lower electronegativity of Ca^{2+} (compared to Mg^{2+}), which allows it to bind more effectively to negatively charged surfaces/functional groups (Gao et al., 2017; Yang et al., 2016). Similar to the monovalent cation conditions, the k_a values of TiO_2 NP were similar in the presence of Mg^{2+} or Ca^{2+} at

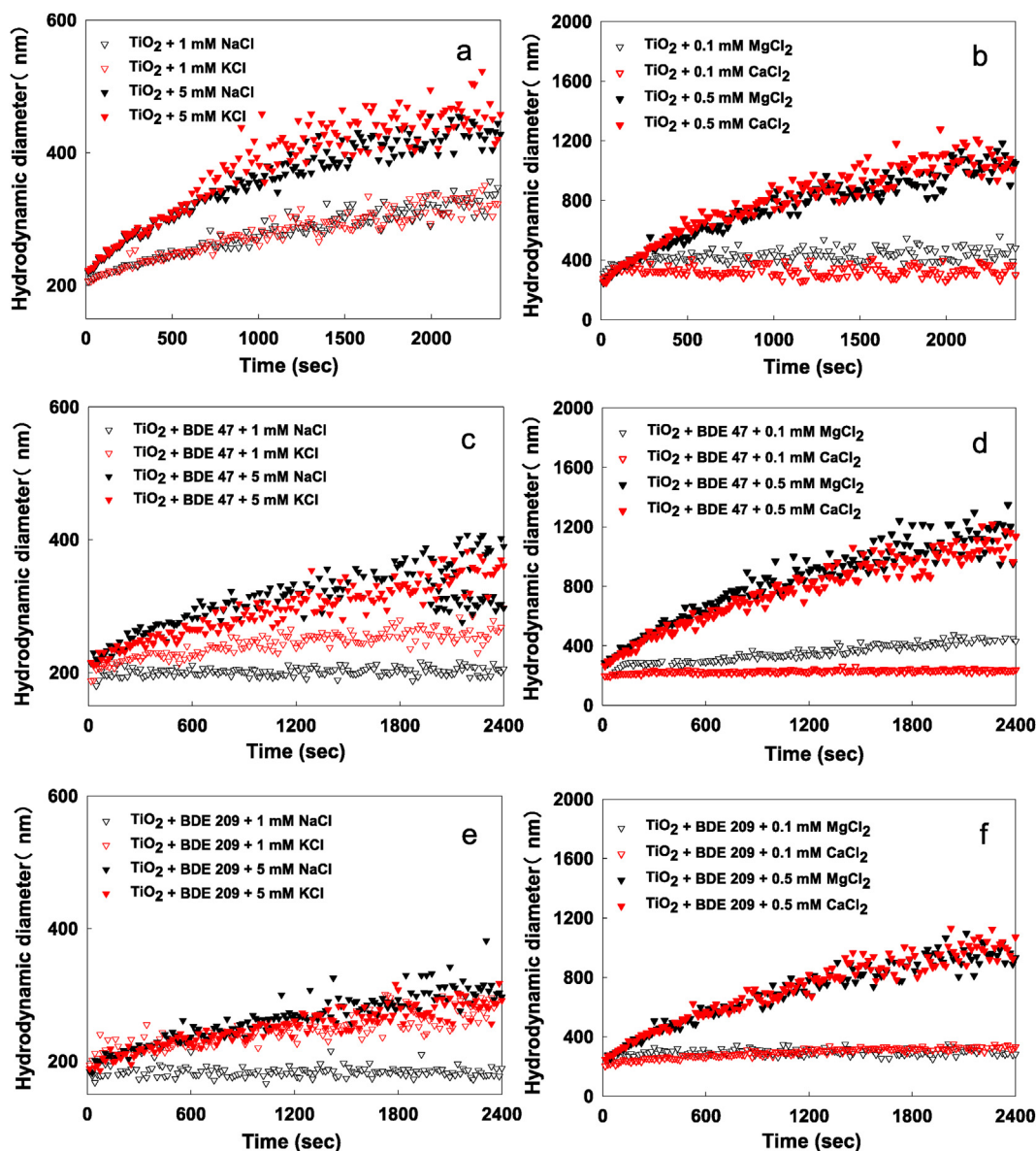


Fig. 7. Effects of BDE 47 and BDE 209 on the agglomeration kinetics of TiO_2 nanoparticles (10 mg/L) in (a, c, e) monovalent ions (1 mM and 5 mM of Na^+ and K^+) and (b, d, f) divalent ions (0.1 mM and 0.5 mM of Ca^{2+} and Mg^{2+}) at pH 7.

0.1 mM (9.7 nm/min and 9.4 nm/min respectively) and 0.5 mM (66.3 nm/min and 68.2 nm/min respectively). The similarities of the initial agglomeration rate of TiO₂ NP at all the conditions tested is probably because TiO₂ NP was experiencing diffusion-limited agglomeration in all the conditions.

A clear suppression of TiO₂ NP agglomeration by the PBDEs was observed in the presence of both monovalent and divalent cations at all the concentrations tested (Figs. 7 and S10). For instance, at 1 mM NaCl, the k_a of TiO₂ NP decreased from 5.9 nm/min without the PBDEs to 0.13 nm/min in the presence of 0.5 mg/L BDE 209 and 0.05 nm/min in the presence of BDE 47. The k_a of TiO₂ NP in the presence of the monovalent ions was much higher in the presence of BDE 209 than in the presence of BDE 47 due to the higher stabilizing ability of BDE 47, as discussed earlier. Similarly, in the presence of the divalent cations, the k_a of TiO₂ NP generally decreased in the presence of the PBDEs, showing the ability of BDE 47 and BDE 209 to stabilize TiO₂ NP in different water chemistry conditions. The trend of improved colloidal stability by the PBDEs in the presence of the divalent ions was not as clear as in the monovalent conditions, possibly due to higher potential of multi-valent ions (and high ionic strengths) to compete for adsorption sites on TiO₂ NP—thereby causing stronger interference of PBDE–TiO₂ interactions.

4. Conclusions

PBDEs are hydrophobic and are thus found dissolved in natural waters at low concentrations. However, TiO₂ NP has a very high surface area, and can adsorb hydrophobic compounds from the aqueous phase. The adsorption of PBDEs may lead to an accumulation of the organic compounds on the surface of TiO₂ NP when released into natural waters (e.g. from sunscreen). The concentration of PBDEs in natural waters is much lower than some of the concentrations considered in this study. We hypothesized that over a long period PBDEs in water will adsorb and concentrate onto the surface of TiO₂ NP. But since this was a short-term study we used higher concentrations of PBDEs to mimic the amount of PBDEs on the surface of TiO₂ NP over a long time. Also, the higher concentrations of PBDEs (such as 5 mg/L) allowed us to “magnify” the effects of PBDEs on TiO₂ NP to understand the mechanism behind the observed effects.

In this study, we showed for the first time that organic contaminants such as PBDEs, which are present in several natural waters also play an important role in the physicochemical properties and environmental fate of TiO₂ NP even in the presence of high content of natural organic matter. The ability of BDE 47 and BDE 209 to suppress the agglomeration of TiO₂ due to electrosteric stabilization was shown in the presence of monovalent and divalent cations. We found that in general, BDE 47 was a better stabilizer of TiO₂ NP when present at the same mass concentration as BDE 209. This improved stability of TiO₂ NP in the presence of BDE 47 reflects its ability to impart a higher surface charge and more effective surface coating of the TiO₂ NP, relative to BDE 209. The aromatic ether groups of PBDEs played an important role in the interactions between the PBDEs and TiO₂ NP. Our observation of improved stability of TiO₂ NP by PBDEs in simple media (DI water with salts) was corroborated by studies carried out in two natural waters (river water and wastewater). Further studies may be needed to clearly see how media pH, and other environmental pollutants impact the ability of PBDEs to interact and stabilize TiO₂ NP in natural waters. The improved stability of PBDE-adsorbed TiO₂ NPs (shown in this study) may result in long-term suspension of TiO₂ NP in natural waters, and lead to enhanced transport of the NPs, especially in surface waters with low salt concentrations.

Acknowledgments

This research was supported by the National Basic Research Program of China (Grant 2015CB459000), the National Natural Science Foundation of China (Project No. 21677078), 111 program, Ministry of Education, China (Grants T2017002).

Appendix A. Supplementary data

Supplementary data related to this article can be found at <https://doi.org/10.1016/j.watres.2018.09.019>.

References

- Adeleye, A.S., Keller, A.A., 2013. Long-term colloidal stability and metal leaching of single wall carbon nanotubes: effect of temperature and extracellular polymeric substances. *Water Res.* 49, 336–250.
- Adeleye, A.S., Conway, J.R., Perez, T., Rutten, P., Keller, A.A., 2014. Influence of extracellular polymeric substances on the long-term fate, dissolution, and speciation of copper-based NPs. *Environ. Sci. Technol.* 48, 12561–12568.
- Adeleye, A.S., Keller, A.A., 2016. Interactions between algal extracellular polymeric substances and commercial TiO₂ NPs in aqueous media. *Environ. Sci. Technol.* 50 (12), 12258–12265.
- Adeleye, A.S., Stevenson, L., Su, Y., Nisbet, R.M., Zhang, Y., Keller, A.A., 2016. Influence of phytoplankton on fate and effects of modified zerovalent iron NPs. *Environ. Sci. Technol.* 50, 5597–5605.
- Ambrosi, A., Chua, C.K., Bonanni, A., Pumera, M., 2012. Lithium aluminum hydride as reducing agent for chemically reduced graphene oxides. *Chem. Mater.* 24, 2292–2298.
- Bettini, S., Boutet-Robinet, E., Cartier, C., Comera, C., Gaultier, E., Dupuy, J., Naud, N., Tache, S., 2017. Food-grade TiO₂ impairs intestinal and systemic immune homeostasis, initiates preneoplastic lesions and promotes aberrant crypt development in the rat colon. *Sci. Rep.* 7, 40373.
- Bouchard, D., Ma, X., Isaacson, C., 2009. Colloidal properties of aqueous fullerenes: isoelectric points and agglomeration kinetics of C₆₀ and C₆₀ derivatives. *Environ. Sci. Technol.* 43, 6597–6603.
- Branchi, I., Capone, F., Alleve, E., Costa, L.G., 2003. Polybrominated diphenyl ethers: neurobehavioral effects following developmental exposure. *Neurotoxicology* (Little Rock) 24, 449–462.
- Chen, K.L., Elimelech, M., 2006. Agglomeration and deposition kinetics of fullerene (C₆₀) NPs. *Langmuir* 22, 10994–11001.
- Chen, M., Xu, N., Cao, X.D., Zhou, K.R., Chen, Z.G., Wang, Y.L., Liu, C., 2015. Facilitated transport of anatase titanium dioxides NPs in the presence of phosphate in saturated sands. *J. Colloid Interface Sci.* 451, 134–143.
- Chowdhury, I., Duch, M.C., Mansukhani, N.D., Hersam, M.C., Bouchard, D., 2013. Colloidal properties and stability of graphene oxide NPs in the aquatic environment. *Environ. Sci. Technol.* 47, 6288–6296.
- Conway, J.R., Adeleye, A.S., Gardea-Torresdey, J.L., Keller, A.A., 2015. Agglomeration, dissolution, and transformation of copper NPs in natural waters. *Environ. Sci. Technol.* 49 (5), 2749–2756.
- Covaci, A., Voorspoels, S., Roosens, L., Jacobs, W., Blust, R., Neels, H., 2008. PBDEs in liver and adipose tissue samples from Belgium. *Chemosphere* 73, 170–175.
- Domingos, R.F., Tufenkji, N., Wilkinson, K.J., 2009. Agglomeration of titanium dioxide NPs: role of a fulvic acid. *Environ. Sci. Technol.* 43 (5), 1282–1286.
- French, R.A., Jacobson, A.R., Kim, B., Isley, S.L., Penn, R.L., Baveye, P.C., 2009. Influence of ionic strength, pH, and cation valence on agglomeration kinetics of titanium dioxide NPs. *Environ. Sci. Technol.* 43 (5), 1354–1359.
- Gao, Y., Ren, X., Tan, X., Hayat, T., Alsaedi, A., Chen, C., 2017. Insights into key factors controlling GO stability in natural surface waters. *J. Hazard Mater.* 335, 56–65.
- Gondikas, A.P., Kammer, F.v.d., Reed, R.B., Wagner, S., Ranville, J.F., Hofmann, T., 2014. Release of TiO₂ NPs from sunscreens into surface waters: a one-year survey at the old danube recreational lake. *Environ. Sci. Technol.* 48 (10), 5415–5422.
- Guzman, K.A.D., Finnegan, M.P., Banfield, J.F., 2006. Influence of surface potential on agglomeration and transport of titania NPs. *Environ. Sci. Technol.* 40 (24), 7688–7693.
- Hale, R.C., Alae, M., Manchester-Neesvig, J.B., Stapleton, H.M., Ikononou, M.G., 2003. Polybrominated diphenyl ether flame retardants in the North American environment. *Environ. Int.* 29, 771–779.
- Her, N.G., Amy, G., Foss, D., Cho, J., 2002. Variations of molecular weight estimation by HP-size exclusion chromatography with UVA versus online DOC detection. *Environ. Sci. Technol.* 36, 3393–3399.
- Hoffmann, M.R., Martin, S.T., Choi, W., Bahnemann, D.W., 1995. Environmental applications of semiconductor photocatalysis. *Chem. Rev.* 9, 69–96.
- Hua, I., Kang, N., Jafvert, C.T., Fábrega-Duque, J.R., 2003. Heterogeneous photochemical reactions of decabromodiphenyl ether. *Environ. Toxicol. Chem.* 22, 798–804.
- Israelachvili, J.N., 2011. *Intermolecular and Surface Forces: Revised, third ed.* Elsevier Science. Academic Press.
- Jallouli, N., Elghniji, K., Trabelsi, H., Ksibi, M., 2014. Photocatalytic degradation of

- paracetamol on TiO₂ NPs and TiO₂/cellulosic fiber under UV and sunlight irradiation. *Arab. J. Chem.* 10, S3640–S3645.
- Kaegi, R., Ulrich, A., Sinnert, B., Vonbank, R., Wichser, A., Zuleeg, S., Simmler, H., Brunner, S., Vonmont, H., Burkhardt, M., Boller, M., 2008. Synthetic TiO₂ NP emission from exterior facades into the aquatic environment. *Environ. Pollut.* 156 (2), 233–239.
- Keller, A.A., Lazareva, A., 2014. Predicted releases of engineered NPs: from global to regional to local. *Environ. Sci. Technol.* 1 (1), 65–70.
- Keller, A.A., McFerran, S., Lazareva, A., Suh, S., 2013. Global life cycle releases of engineered NPs. *J. Nanoparticle Res.* 15 (6), 1–17.
- Keller, A.A., Wang, H., Zhou, D., Lenihan, H.S., Cherr, G., Cardinale, B.J., Miller, R., Ji, Z., 2010. Stability and agglomeration of metal oxide NPs in natural aqueous matrices. *Environ. Sci. Technol.* 44 (6), 1962–1967.
- Lambert, J.B., Shurvell, H.F., Cooks, R.G., 1987. *Introduction to Organic Spectroscopy*. Macmillan, New York.
- Leenheer, J.A., Croué, J.P., 2003. Peer reviewed: characterizing aquatic dissolved organic matter. *Environ. Sci. Technol.* 37 (1), 18A–26A.
- Li, S.C., Chu, L.N., Gong, X.Q., Diebold, U., 2010. Hydrogen bonding controls the dynamics of catechol adsorbed on a TiO₂ (110) surface. *Sci. Technol. Humanit.* 328 (5980), 882–884.
- Li, Y., Yang, N., Du, T., Xia, T., Zhang, C., Chen, W., 2016. Chloramination of graphene oxide significantly affects its transport properties in saturated porous media. *Nanoimpact* 3–4, 90–95.
- Lin, D., Story, D., Walker, S.L., Huang, Q., Liang, W., Cai, P., 2017. Role of pH and ionic strength in the agglomeration of TiO₂ NPs in the presence of extracellular polymeric substances from *Bacillus subtilis*. *Environ. Pollut.* 228, 35–42.
- Lin, D., Story, S.D., Walker, S.L., Huang, Q.Y., Cai, P., 2016. Influence of extracellular polymeric substances on the agglomeration kinetics of TiO₂ NPs. *Water Res.* 104, 381–388.
- Moon, H.B., Kannan, K., Lee, S.J., Choi, M., 2007. Atmospheric deposition of polybrominated diphenyl ethers (PBDEs) in coastal areas in Korea. *Chemosphere* 66, 585–593.
- Ni, S., Cui, Q., Zheng, Z., 2014. Interaction of polybrominated diphenyl ethers and aerobic granular sludge: biosorption and microbial degradation. *BioMed Res. Int.* 291, 274620.
- Peng, X., Tang, C., Yu, Y., Tan, J., Huang, Q., Wu, J., Chen, S., Ma, B., 2009. Concentrations, transport, fate, and releases of polybrominated diphenyl ethers in sewage treatment plants in the Pearl River Delta, South China. *Environ. Int.* 35, 303–309.
- Peng, Y., Chen, M., Shih, Y., 2013. Adsorption and sequential degradation of polybrominated diphenyl ethers with zerovalent iron. *J. Hazard. Mater.* 260, 844–850.
- Priester, J.H., Van De Werfhorst, L.C., Ge, Y., Adeleye, A.S., Tomar, S., Tom, L.M., Piceno, Y.M., Andersen, G.L., Holden, P.A., 2014. Effects of TiO₂ and Ag NPs on polyhydroxybutyrate biosynthesis by activated sludge bacteria. *Environ. Sci. Technol.* 48 (24), 14712–14720.
- Qi, Y., Xia, T., Li, Y., Duan, L., Chen, W., 2016. Colloidal stability of reduced graphene oxide materials prepared using different reducing agents. *Environ. Sci. Nano.* 3, 1062–1071.
- Song, R., Qin, Y., Suh, S., Keller, A.A., 2017. Dynamic model for the stocks and release flows of engineered nanomaterials. *Environ. Sci. Technol.* 51 (21), 12424–12433.
- Tittlemier, S.A., Halldorson, T., Stern, G., Tomy, G.T., 2002. Vapor pressures, aqueous solubilities, and Henry's law constants of some brominated flame retardants. *Environ. Toxicol. Chem.* 21 (9), 1804–1810.
- U.S. Environmental Protection Agency (EPA), 2010. *An Exposure Assessment of Polybrominated Diphenyl Ethers*. National Center for Environmental Assessment, Washington, DC. EPA/600/R-08/086F.
- Vargas, R., Núñez, O., 2009. Hydrogen bond interactions at the TiO₂ surface: their contribution to the pH dependent photo-catalytic degradation of p-nitrophenol. *J. Mol. Catal. Chem.* 300 (1), 65–71.
- Vittadini, A., Selloni, A., Rotzinger, F.P., Grätzel, M., 2000. Formic acid adsorption on dry and hydrated TiO₂ anatase (101) surfaces by DFT calculations. *J. Phys. Chem. B* 104 (6), 1300–1306.
- Wang, H., Adeleye, A.S., Huang, Y., Li, F., Keller, A.A., 2015. Heteroagglomeration of NPs with biocolloids and geocolloids. *Adv. Colloid Interface Sci.* 226, 24–36.
- Wang, P., Qi, N., Ao, Y., Hou, J., Wang, C., Qian, J., 2016. Effect of UV irradiation on the agglomeration of TiO₂ in an aquatic environment: influence of humic acid and pH. *Environ. Pollut.* 212, 178–187.
- Yang, K., Chen, B., Zhu, X., Xing, B., 2016. Agglomeration, adsorption and morphological transformation of graphene oxide in aqueous solutions containing different metal cations. *Environ. Sci. Technol.* 50, 11066–11075.
- Zhou, D., Ji, Z., Jiang, X., Dunphy, D.R., Brinker, C.J., Keller, A.A., 2013. Influence of Material Properties on TiO₂ NP Agglomeration. *PLoS One* 8 (11), e81239.
- Zhu, L.Y., Hites, R.A., 2004. Temporal trends and spatial distributions of brominated flame retardants in fishes from the great lakes. *Environ. Sci. Technol.* 38, 2779–2784.
- Zhang, X., Luo, X., Chen, S., Wu, J., Mai, B., 2009. Spatial distribution and vertical profile of polybrominated diphenyl ethers, tetrabromobisphenol A, and decabromodiphenylethane in river sediment from an industrialized region of South China. *Environ. Pollut.* 157, 1917–1923.